J Therm Anal Calorim (2015) 119:1381–1391
DOI 10.1007/s10973-014-4287-0

Synthesis, characterization, and thermal degradation kinetics of biuret–formaldehyde polymeric ligand and its polymer metal complexes

Naushad Ahmad · Manawwer Alam · Mshari Ayad N. Alotaibi

Received: 16 May 2014 / Accepted: 4 November 2014 / Published online: 30 November 2014

Abstract In the present study, biuret–formaldehyde (BF) polymeric ligand was prepared by condensation reaction, and its polymer metal complexes [BF-M(II)] were prepared with transition metal ions. Synthesized polymers were characterized by elemental, spectral, and thermal analyses. The geometry of central metal ions was determined using magnetic susceptibility measurement and electronic spectra, which reveals that Co(II) and Ni(II) ions have octahedral geometry, while Cu(II) and Zn(II) ions have square planer and tetrahedral geometry, respectively. Thermogravimetric (TG) analysis was used to estimate thermal and kinetic behavior of polymers at heating rates of 10, 15, and 20 °C min^{-1} under helium atmosphere. The TG curves of polymers at three heating rates were more or less in similar shape, which indicated that mass loss is independent of heating rate. Thermogravimetric data were analyzed by means of model-free isoconversional method of Flynn–Wall–Ozawa and Kissinger–Akahira–Sunose on the whole range of temperature. It was found that values of apparent activation energy (E_a) of [BF-M(II)] polymers are higher than BF and influenced by the metal type.

N. Ahmad (✉)
Department of Chemistry, King Saud University,
P.O. Box 2455, Riyadh 11451, Kingdom of Saudi Arabia
e-mail: naushaddrnaima@gmail.com

M. Alam
Research Center-College of Science, King Saud University,
P.O. Box 2455, Riyadh 11451, Kingdom of Saudi Arabia

M. A. N. Alotaibi
Department of Chemistry, College of Science, Salman bin Abdulaziz University, Al-Kharj, Kingdom of Saudi Arabia

Keywords Biuret–formaldehyde · Thermogravimetric analysis · Decomposition kinetics

Introduction

Polymers with functional groups are prime research area of material science for the investigating thermal, kinetics, optical, and mechanical properties [1, 2]. Coordination of metal ions with polymeric systems containing nitrogen, oxygen, and sulfur donor atoms/groups is a very important class of polymer, which impart both flexibility owing to organic moiety and thermal stability as a consequence of metal ions in the same polymeric frame [2–4]. They play an essential role in various fields of material science, metallurgy, environmental protection, and thermochemistry. They also have great advantage over organic polymer and widely used in many specified fields such as conductivity, luminescence, thermal insulation, catalysis, magnetism, nonlinear optics, and coating materials [5]. Several formaldehyde resins such as urea–formaldehyde, thiourea–formaldehyde, semicarbazide–formaldehyde, thiosemicarbazide–formaldehyde, phenylurea–formaldehyde show signs of good adhesive system for the production of interior grade wood-based panels, higher thermal stability, and greater antimicrobial activities [6–9]. The main advantages of formaldehyde resins are good reactivity and water solubility, and poor resistance to moisture and water, which make them very suitable for interior applications. The reaction mechanism and kinetics of these polymers is challenging and difficult task with complexity results from great variety of factors with diverse effects. Thermogravimetric (TG) analysis, differential scanning calorimetry (DSC), and differential thermal (DT) analysis have the great advantageous and provide vital information about physico-

chemical parameters of materials [10]. The consequences obtained with application of thermal analyses and use of various kinetic models can be supportive in material science for studying thermal behavior and kinetic of solid-state reactions [11]. For gaining value of apparent activation energy, which is the most probable mechanism functions/models of reaction, a variety of methods, isoconversional and non-isoconversional, were described in literatures such as the Flynn–Wall–Ozawa (FWO) [12, 13], Kissinger–Akahira–Sunose (KAS) [14, 15], Friedman [16], and Coats and Redfern [17]. These methods have been widely used to kinetics study of chemical or physical processes, and allow drawing important information about mechanisms of various chemical reactions, cross-linking, polymer crystallization, and glass transition kinetics [18–20].

Formaldehyde base polymers can be synthesized by applying different reaction conditions and preparation methods in order to meet the requirements of specific application. In present study, we report synthesis of biuret–formaldehyde as a polymeric ligand and its polymer metal complexes with transition metal ions. The synthesized polymers have been characterized by elemental, spectral, and thermal analysis. The kinetics analyses of non-isothermal TG data of synthesized polymers have been evaluated by means of the integral isoconversional methods of FWO and KAS, which was reported for the first time.

Theory for kinetic analysis

TG/DTG technique is very useful for the determination of decomposition temperature, decomposition steps, and kinetics triplet for solid substances. Isoconversional methods in non-isothermal TG experiments are valuable for kinetics parameter evaluation. These methods have been recommended by International Confederation of Thermal Analysis Calorimetry (ICTAC) due to the fact that they allow calculating the apparent activation energy independently [21, 22]. It is a model-free method, which involves determining temperatures of decomposition reaction corresponding to fixed values (α) at different heating rates (β) from TG experiments. The kinetics of thermal alteration of a polymer is generally expressed by the following equation:

$$v = \left(\mathrm{d}\alpha/\mathrm{d}t\right) = k(T)f(\alpha) = A\exp((-E_\mathrm{a})/RT)f(\alpha), \qquad (1)$$

where $\mathrm{d}\alpha/\mathrm{d}t$ is the reaction rate, α is the degree of conversion, t is the reaction time, T is the absolute temperature of reaction, A is the pre-exponential (frequency) factor, measure the probability of a molecule that having apparent activation energy E_a, and R is the universal gas constant (8.314 J mol^{-1} K^{-1}). The parameters of reaction kinetics are determined using the following procedure: under non-isothermal conditions in which a sample is heated at a constant rate. By introducing linear heating rate of $\beta = \mathrm{d}T/\mathrm{d}t$ (K/s), in Eq. (1),

$$(\mathrm{d}\alpha/\mathrm{d}T) = (A/\beta)f(\alpha)\exp((-E_\mathrm{a})/RT). \qquad (2)$$

This is a fundamental equation of non-isothermal solid kinetics. In the present study, apparent activation energy can be calculated by two isoconversional integral methods, FWO [12, 13] and KAS [14, 15].

The FWO method is one of isoconversional model-free integral methods that can determine apparent activation energy without knowledge of reaction order. Equation (2) is integrated using the Doyle approximation [23]. The result of integration after taking natural logarithms is

$$\ln\beta = -1.052(E_\alpha/RT) + \ln(AE_\alpha)/R) - \ln g(\alpha) - 5.3305\,], \qquad (3)$$

where β, A, E_a, and T have known meanings. $g(\alpha)$ is integral form of $f(\alpha)$, which is the reaction model that depends on reaction mechanism. The E_a for different conversion values can be calculated from ln β versus $1000/T$ plot. In this case, conversion dependence function ($f(\alpha)$ or $g(\alpha)$) is not required. Another expression similar to a proposal by FWO is KAS method based on the Coats–Redfern [17] approximation, which is described by the following equation:

$$\ln(\beta/T^2) = \ln[AR/Eag(\alpha)] - E_\alpha/RT. \qquad (4)$$

For constant α, a plot of ln β/T^2 versus $1000/T$ is a straight line whose slope is E_a/RT.

Experimental

Materials and measurements

Biuret, formaldehyde (37 % aqueous solution), NaOH (40 % aqueous solution), $CoCl_2{\cdot}6H_2O$, $NiCl_2{\cdot}6H_2O$, $CuCl_2{\cdot}2H_2O$, and $ZnCl_2$ obtained as reagent grade from Sigma Aldrich, USA are used as received. Solvents like DMF, DMSO, EtOH, MeOH, diethyl ether, and acetone (Fluka USA) were used without further purification.

Elemental analyses were carried out using Perkin–Elmer 2400 Series II, CHNS/O Analyzer. The metal percentages were determined by complexometric titration against EDTA after decomposing with mixture of HCl and $HClO_4$. The FT-IR spectra were recorded over 4,000–400 cm^{-1} range on a Bruker Tensor 27 FT-IR spectrophotometer using KBr pellets. NMR (^{1}H NMR and ^{13}C NMR) spectra were recorded on a JEOL-GSX 300-MHz FX-1000 FT-NMR at room temperature using deuterated DMSO as a solvent and TMS as an internal standard. Electronic spectra were recorded on a Perkin–Elmer Lambda-25 UV–Vis spectrometer using

Table 1 Elemental analysis data of polymeric ligand and its polymer metal complexes

Compounds	Yield/%	Color	Elemental analysis[a]			
			Carbon	Hydrogen	Nitrogen	Metal
BF $(C_6H_{10}O_4N_6)_n$	79.39	White	30.03/31.31	4.93/4.38	33.62/34.51	–
BF-Co(II) $(C_6H_8O_4N_6Co)_n$	73.05	Dark brown	28.67/27.10	2.39/2.41	28.56/29.03	19.98/20.13
BF-Ni(II) $(C_6H_8O_4N_6Ni)_n$	70.12	Grayish brown	24.84/25.12	2.74/2.81	28.93/29.30	21.06/20.56
BF-Cu(II) $(C_6H_8O_4N_6Cu)_n$	68.09	Green	23.19/24.08	2.89/2.76	28.37/28.81	20.17/21.38
BF-Zn(II) $(C_6H_8O_4N_6Zn)_n$	65.03	White	24.71/24.55	3.04/2.85	27.55/28.13	22.89/22.48

[a] The calculated/found values

DMSO as solvent. The magnetic susceptibility measurement at room temperature was carried out by Gouy's method using $Hg[Co(NCS)_4]$ as reference. Thermal behaviors of synthesized polymers were carried out by TGA/DSC1 (Mettler Toledo AG, Analytical CH-8603, Schwerzenbach, Switzerland) in helium atmosphere (50 mL min^{-1}) at heating rate, $\beta = 10$, 15, and 20 °C min^{-1}, in temperature range from ambient temperature to 800 °C, and uniformity of sample (0.5 ± 0.005 mg) was maintained by spreading it uniformly over crucible base in all the experiments. The sample temperature, which is controlled by a thermocouple, did not exhibit any systematic deviation from preset linear temperature programs. Duplicate run was made under similar conditions and found that data overlap with each other, indicating satisfactory reproducibility.

Synthesis of polymeric ligand (BF)

Biuret (0.05 mol) and 37 % aqueous solution of formaldehyde (3.75 mL, 0.05 mol) were mixed in 50 mL of deionized H_2O in a three-necked round-bottom flask equipped with a water-cooled condenser, thermometer, and magnetic stirrer. The pH of solution was adjusted at 8.5 using 40 % aqueous solution of NaOH. The mixture was heated at 70 °C for 6 h; progress of reaction was monitored using thin layer chromatography (TLC). The final mixture was cooled, and pH of reaction mixture was adjusted using HCl solution; solid white precipitate of BF was obtained, which was filtered and washed several times with water, acetone, and dried in vacuum oven for overnight.

Synthesis of polymer metal complexes [BF-M(II)]

Biuret–formaldehyde (0.05 mol) was dissolved in DMSO and heated at 70 °C in a round-bottom flask. $CoCl_2{\cdot}6H_2O$ (0.05 mol) dissolved in DMSO was added to hot solution and heated for 5 h at same temperature. Stirring was continued until complete dissolution, and distinct color change was achieved. Finally, a dark brown, sticky product was obtained. This sticky product was precipitated in deionized water. The obtained brown precipitate was filtered and washed several times with acetone and diethyl ether. The product was dried in a vacuum oven at 70 °C, which gave a grayish brown precipitate and yield 73.05 %. Similar procedures were applied for the preparation of Ni(II), Cu(II), and Zn(II) polymer metal complexes, and yields and color are given in Table 1.

Results and discussion

The polymeric ligand has been synthesized by the methylolation process in alkaline medium followed by condensation polymerization reactions between formaldehyde and biuret. Subsequent addition of biuret proceeds in one or more stages during the acid condensation stage. Finally, the reaction mixture is cooled down, and water is removed in order to obtained good yield. The polymer metal complexes were prepared by reaction of polymeric ligand with divalent transition metal ions Co(II), Ni(II), Cu(II), and Zn(II) as shown in Scheme 1. The prepared compounds have been characterized by elemental analysis, FT-IR, UV–visible, NMR (^{1}H NMR and ^{13}C NMR) spectra as well as thermal analysis. The analytical data shown in Table 1, a slight deviation in elemental analysis, may be due to polymeric nature of compounds. It was also observed through analytical data BF-Co(II) and BF-Ni(II) which were coordinated with two molecules of water but BF-Cu(II) and BF-Zn(II) did not have coordinated water which was supported by the electronic spectra and TG results.

Scheme 1 Synthesis of biuret–formaldehyde polymeric ligand (BF) and its polymer metal complexes

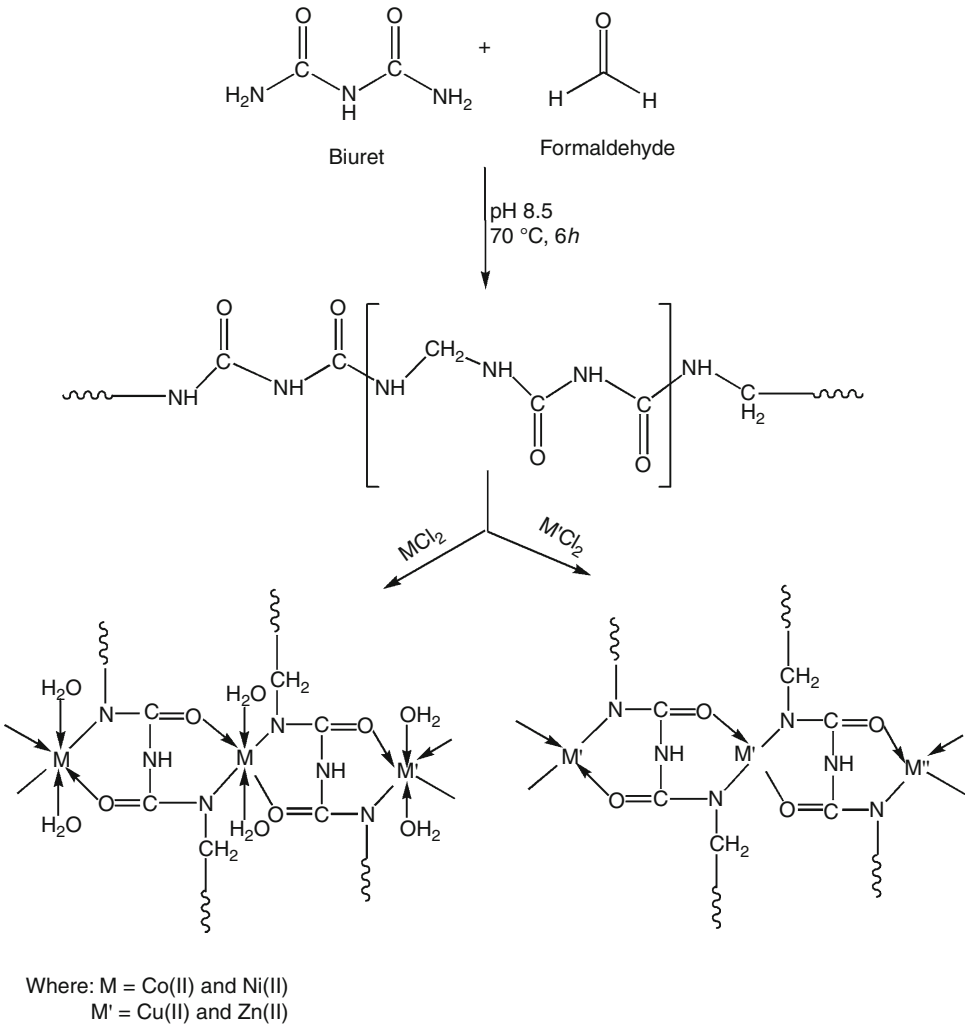

Table 2 FT-IR spectral data of polymeric ligand and its polymer metal complexes

Compound	OH	C=O	C–H	C–N	M–O	M–N
BF	3,220	1,685	1,480	1,285	–	–
BF-Co(II)	3,364	1,654	1,458	1,250	551	520
BF-Ni(II)	3,383	1,646	1,405	1,230	582	525
BF-Cu(II)	3,385	1,635	1,450	1,215	578	515
BF-Zn(II)	3,370	1,650	1,434	1,261	585	530

FT-IR spectra

The FT-IR spectra of BF and BF-M(II) with their assignments are summarized in Table 2. In the spectrum of polymeric ligand, a very broad band is observed in 3,358 cm^{-1} due to N–H [24]. The presence of methylene group is confirm by appearance of two strong bands at 2,934, 2,895 cm^{-1} of CH_2 asymmetric, symmetric stretching, and a band at 1,465 cm^{-1} due to CH_2 bending mode [6]. A sharp absorption band at 1,285 cm^{-1} is attributed to C–N bending. The C=O stretching frequency of BF appears at 1,685 cm^{-1}, while in BF-M(II), a major shift to lower wave number by 25–30 cm^{-1}. The presence of coordination water molecules in spectra of BF–Co(II) and BF–Ni(II) was supported by appearance of absorption bands at 3,330–3,310 cm^{-1} for O–H vibration and between 670–650 for rocking mode of coordination water [25], while these bands were disappeared in spectra of BF-Cu(II) and BF-Zn(II). The appearance of two new bands in IR spectra of polymer metal complexes around 610–590 and 510–490 cm^{-1} were observed due to coordination of metal ions with carbonyl oxygen (M–O) and amide nitrogen (M–N), respectively [26, 27].

^{1}H and ^{13}C NMR spectra

The protons of amide NH resonance signals appear at 6.03 ppm and 9.87 ppm corresponding to CH_2–N**H**–C=O and O=C–N**H**–C=O, respectively. The methylene group

Table 3 Magnetic moment and electronic spectral data of polymer metal complexes

Compound	μ_{eff}/B.M.	Frequency/cm^{-1}	Assignments	Δ_o/cm^{-1}	B/cm^{-1}	β	Geometry
BF-Co(II)	4.2	8,857	$^4T_{2g}(F) \leftarrow {}^4T_{1g}(F)$ (v_1)	11,070	738	0.658	Octahedral
		17,428	$^4A_{2g}(F) \leftarrow {}^4T_{1g}(F)$ (v_2)				
		19,480	$^4T_{1g}(P) \leftarrow {}^4T_{1g}(F)$ (v_3)				
BF-Ni(II)	3.4	8,573	$^3T_{2g}(F) \leftarrow {}^3A_{2g}(F)$ (v_1)	9,351	779	0.721	Octahedral
		15,998	$^3T_{1g}(F) \leftarrow {}^3A_{2g}(F)$ (v_2)				
		24,018	$^3T_{1g}(P) \leftarrow {}^3A_{2g}(F)$ (v_3)				
BF-Cu(II)	2.1	14,987	$^2A_{1g} \leftarrow {}^2B_{1g}$				Square planar
		24,440	Charge transfer				

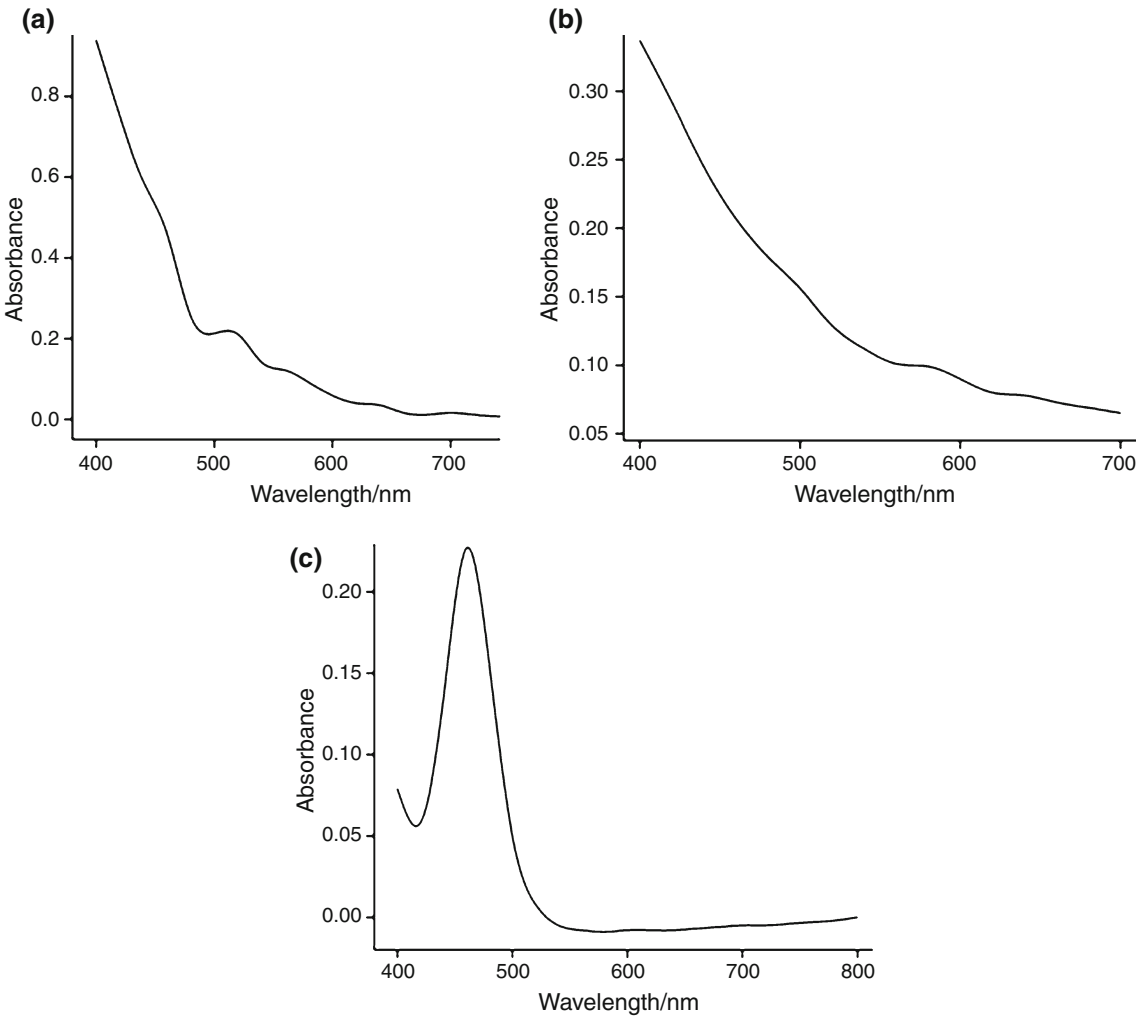

Fig. 1 Electronic spectra of **a** BF-Co(II), **b** BF-Ni(II), and **c** BF-Cu(II) polymer metal complexes

(NH–C**H**$_2$–NH) of synthesized polymeric ligand shows resonance signal at 4.89 ppm. In the spectrum of BF–Zn(II), amide proton (CH_2–N**H**–C=O) resonance at 6.03 ppm was disappeared because of deprotonation of BF with metal ions and support coordination [28]. On the other hand, methylene protons of BF-Zn(II) were also shifter toward downfield and appear at 3.68 ppm.

In the ^{13}C NMR spectra of BF and BF-Zn(II) complex, signals for **C**H_2 group of NH–**C**H_2–NH appear at 60.12 ppm and 63.02 ppm respectively. The resonance

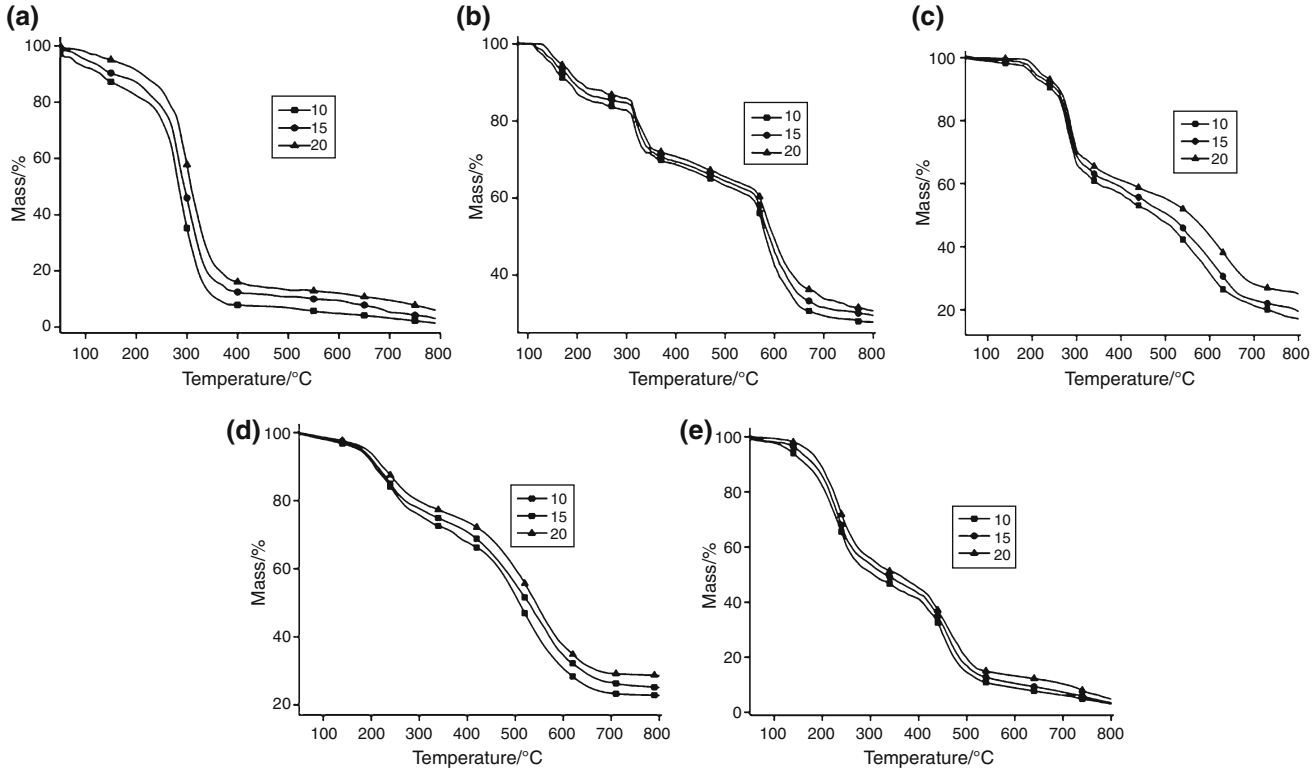

Fig. 2 TG curves of **a** BF, **b** BF-Co(II), **c** BF-Ni(II), **d** BF-Cu(II), and **e** BF-Zn(II) recorded at different heating rates of 10, 15, and 20 °C min^{-1}

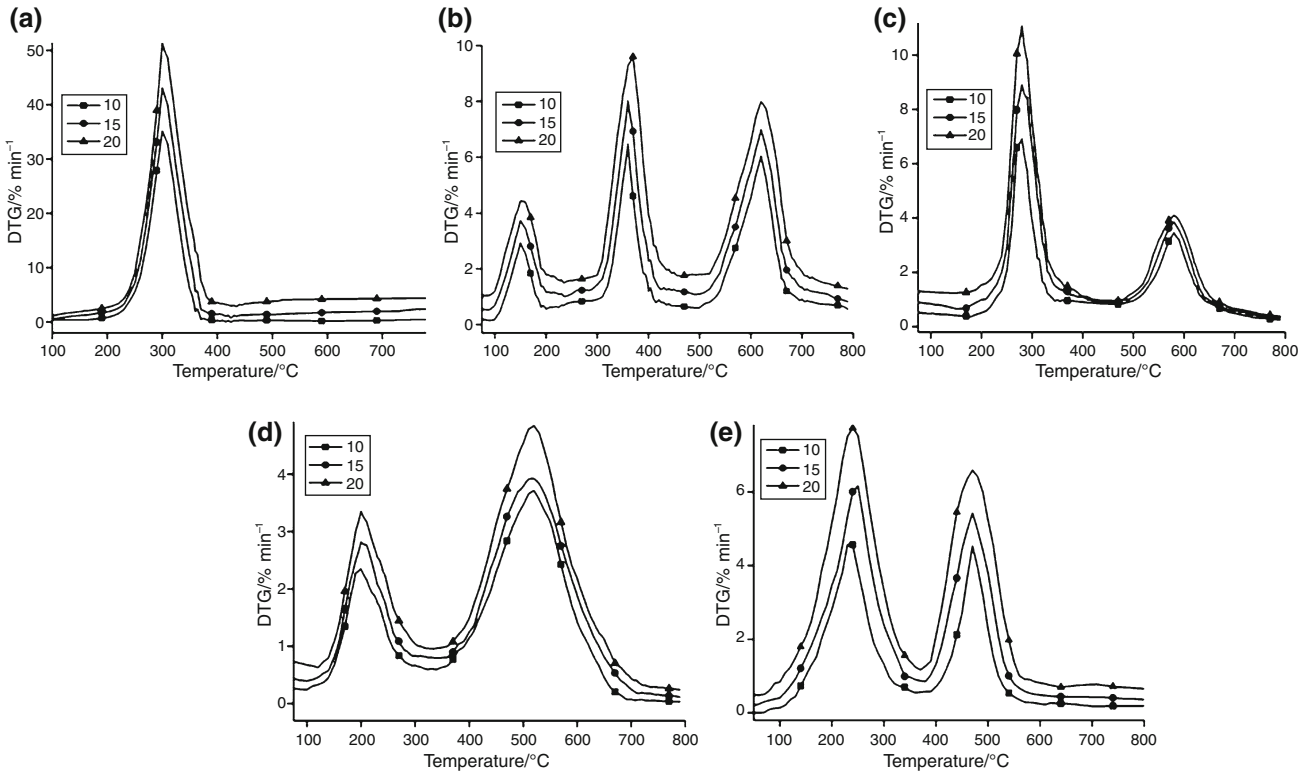

Fig. 3 DTG curves for thermal decomposition process of **a** BF, **b** BF-Co(II), **c** BF-Ni(II), **d** BF-Cu(II), and **e** BF-Zn(II) recorded at different heating rates of 10, 15, and 20 °C min^{-1}

Table 4 DTG phenomenological data of polymeric ligand and its polymer metal complexes at three heating rates

Heating rate	BF		BF-Co(II)					BF-Ni(II)					BF-Cu(II)			BF-Zn(II)		
	T_{max1}	α_{max1}	T_{max1}	α_{max1}	T_{max2}	α_{max2}	T_{max3}	α_{max3}	T_{max1}	α_{max1}	T_{max2}	α_{max2}	T_{max1}	α_{max1}	T_{max2}	α_{max2}	T_{max1}	α_{max1}	T_{max2}	α_{max2}
10	301.4	34.6	150.0	2.78	359.3	6.2	623.2	5.9	276.5	7.2	579.3	3.3	199.2	2.3	517.7	3.6	230.5	4.5	467.7	4.3
15	303.3	42.3	154.6	3.63	362.1	7.9	625.1	6.2	279.3	8.8	581.2	3.7	205.2	2.8	519.1	3.9	237.7	5.9	469.6	5.2
20	307.2	51.1	158.3	4.45	370.2	9.5	627.5	7.8	284.4	10.9	589	4.1	208.3	3.3	521.9	4.8	242.9	7.6	473.1	6.5

signal around 157.23 ppm is assigned to carbonyl carbon of polymeric ligand [29]. A downfield shift of carbonyl carbon signal in case of diamagnetic metal complex is an indication of complexation process viz a significant carbonyl $C^{\delta+}\ldots O^{\delta-}$ contribution to stability of complexes, and resultant reduction in the electron density and appears at 153.04 ppm. It is also examined for both (^{1}H NMR and ^{13}C NMR) spectra that solvent (DMSO) did not have any coordinating effect in spectra of BF and its Zn(II) metal complex.

UV–Visible analysis and magnetic studies

Electronic spectra BF-M(II) were recorded in DMSO solution (10^{-3} M), and various crystal field parameters such as Δ_o, Racah parameter (B), and Nephelauxetic parameter (β) have been calculated and tabulated in Table 3. The Nephelauxetic parameter β was obtained using the relation

$$\beta = \mathrm{B\ (complex)/B(free\ ion)}. \quad (5)$$

The BF-Co(II) has magnetic moment 4.27 BM and showed three absorption bands at 8,857, 17,428, and 19,480 cm^{-1} due to $^{4}T_{2g}(F) \leftarrow {}^{4}T_{1g}(F)$ (ν_1), $^{4}A_{2g}(F) \leftarrow {}^{4}T_{1g}(F)$ (ν_2), and $^{4}T_{1g}(P) \leftarrow {}^{4}T_{1g}(F)$ (ν_3) transitions, respectively, which is indicated an octahedral environment around Co(II) ion (Fig. 1a) [30]. The crystal field parameters of this polymer metal complex were $\Delta_o = 11{,}070\ cm^{-1}$, $B = 738\ cm^{-1}$, and $\beta = 0.658$. The reduction of Racah parameter from free ion values of 1,120–738 cm^{-1} and value of β indicate the presence of a covalence nature of complex.

The magnetic moment of BF-Ni(II) is 3.4 BM and showed three absorption bands at 8,573, 15,998, and 24,102 cm^{-1} which correspond to $^{3}T_{2g}(F) \leftarrow {}^{3}A_{2g}(F)$ (ν_1), $^{3}T_{1g}(F) \leftarrow {}^{3}A_{2g}(F)$ (ν_2), and $^{3}T_{1g}(P) \leftarrow {}^{3}A_{2g}(F)$ (ν_3) transitions, respectively. The crystal field parameters were $\Delta_o = 9351\ cm^{-1}$, $B = 779\ cm^{-1}$, and $\beta = 0.721$ which is favor of an octahedral geometry for Ni(II) ions (Fig. 1b) [31]. The reduction free ion value of 1,080 to 779 cm^{-1} and β value of 0.721 indicate covalent nature of compound.

The magnetic moment of Cu(II) complex is 2.10 BM and showed two energy bands at 14,987 and 24,440 cm^{-1}, which assigned to $^{2}A_{1g} \leftarrow {}^{2}B_{1g}$ and charge transfer band that indicated a square planar geometry (Fig. 1c) [32]. Thus, electronic spectral studies further supported structure of proposed Scheme 1.

TG data analysis

The TG curves for BF and its BF-M(II) polymers at various heating rates are shown in Fig. 2, which present mass loss during heating from ambient temperature to 800 °C. BF-

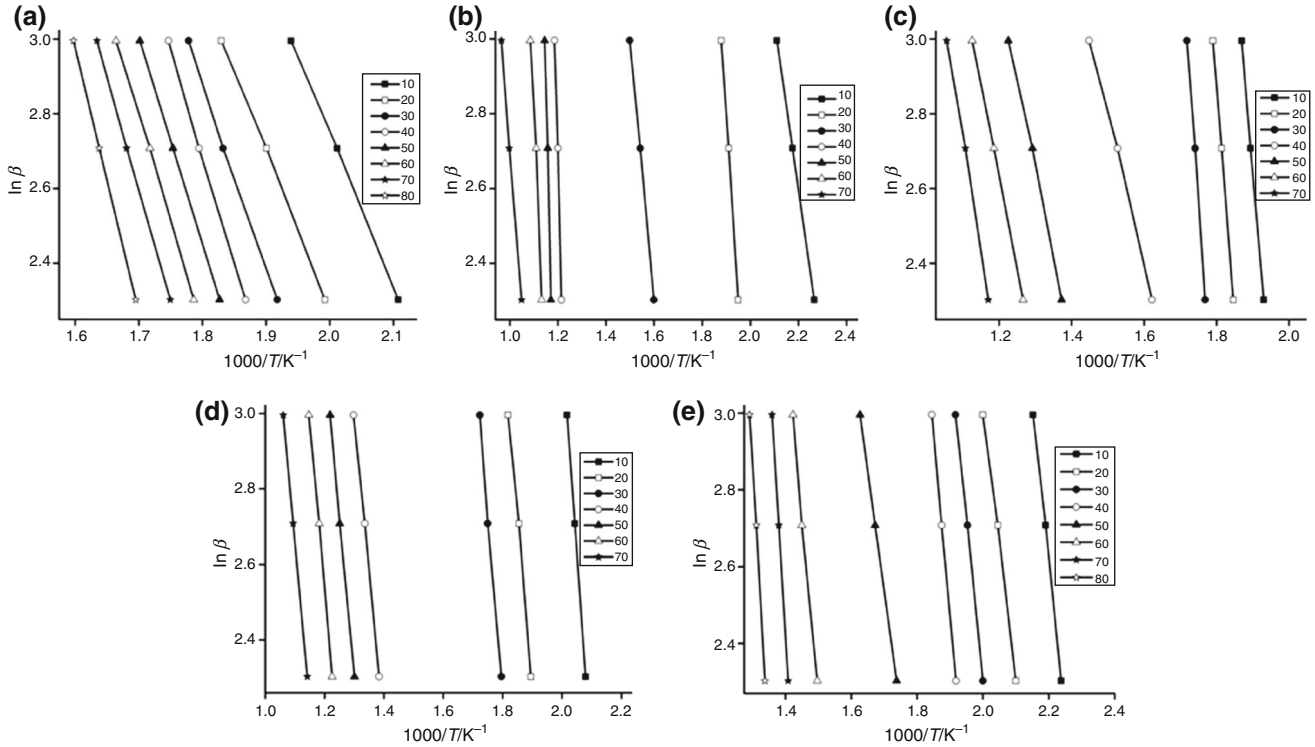

Fig. 4 Isoconversional plots for **a** BF, **b** BF-Co(II), **c** BF-Ni(II), **d** BF-Cu(II), and **e** BF-Zn(II) by FWO method

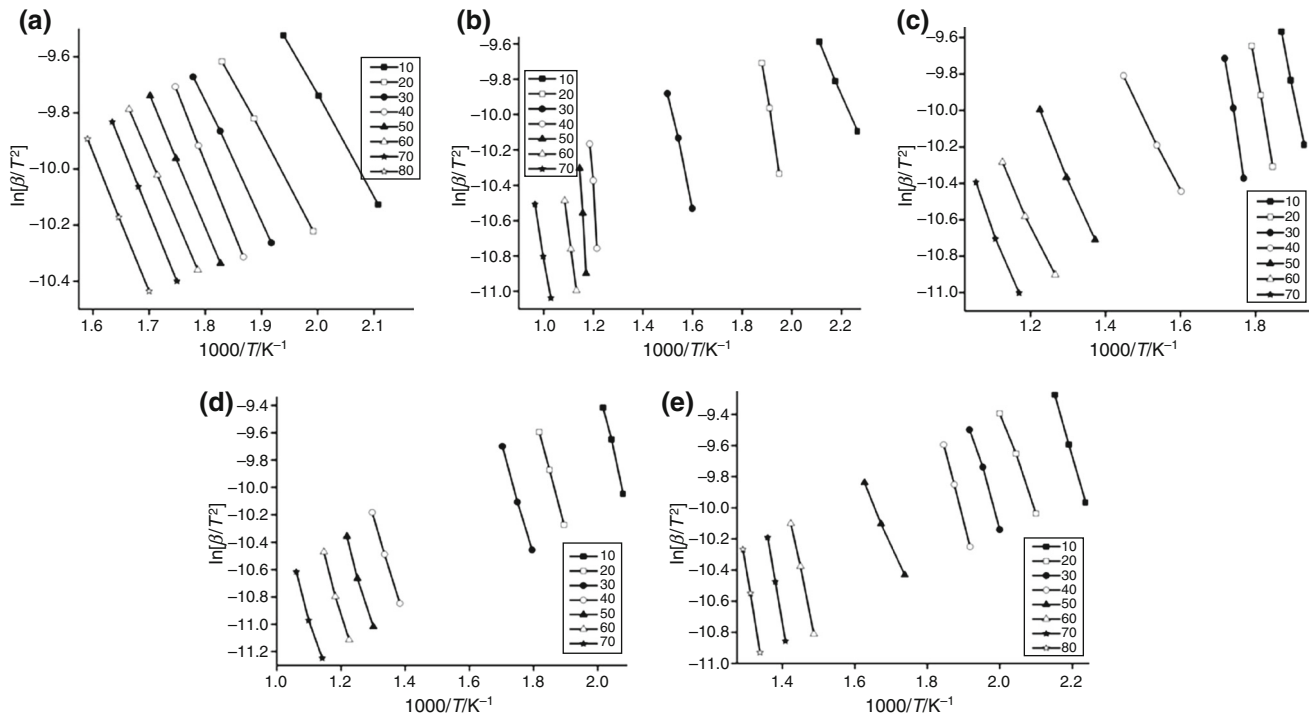

Fig. 5 Isoconversional plots for **a** BF, **b** BF-Co(II), **c** BF-Ni(II), **d** BF-Cu(II), and **e** BF-Zn(II) by KAS method

M(II) polymers show relatively good thermal stability, due to initially small mass loss ($\sim$1 %), at $\sim$50 °C. The initial minor mass loss is related to loss of moisture and trapped solvent, while major mass loss is due to decomposition organic and inorganic parts of polymers in various steps. As can be seen in Fig. 2, there is a shift in TG curves

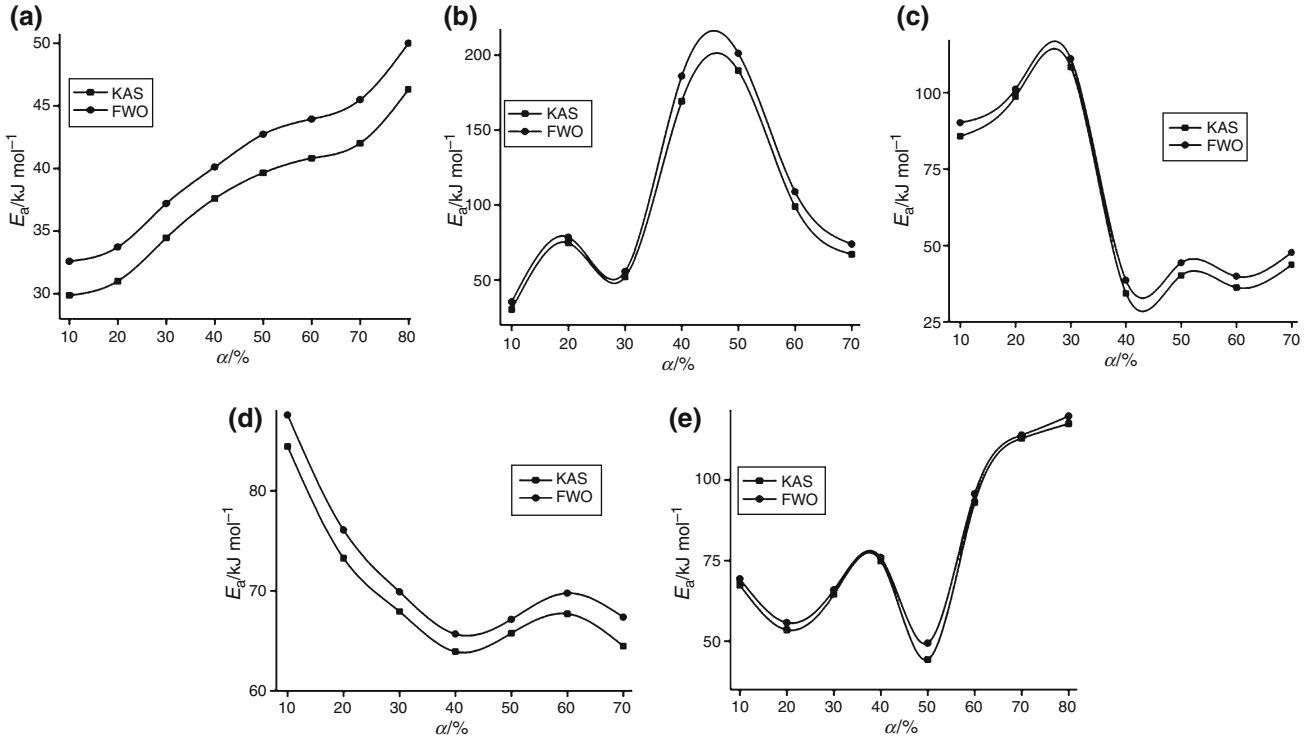

Fig. 6 The apparent activation energy, E_a, plotted as a function of the degree of conversion, α, for the **a** BF, **b** BF-Co(II), **c** BF-Ni(II), **d** BF-Cu(II), and **e** BF-Zn(II) by FWO and KAS method

caused by increasing heating rates. All TG curves are approximately in same shape indicating that mass loss is independent of heating rate, and mass loss increases with decreasing of heating rate. The corresponding DTG curves are presented in Fig. 3, which represent rate of mass loss $d\alpha/dt$ curves during heating from ambient temperature to 800 °C. The peaks in DTG curves directly correspond to mass loss observed on TG curves. The maximum rate of mass loss α_{max} (% min^{-1}) at peak temperature T_{max} (°C) determined from DTG curves at constant heating rate β (°C min^{-1}) is presented in Table 4, and the peak temperature shifts to higher temperature as heating rate increases from 10 to 20 °C min^{-1}. The subscripts 1, 2, and 3 represent the first, second, and third step of degradation, respectively. The DTG curves reveal different profiles for BF and its BF-M(II) polymers depending on heating rates and type of metal ions. Figure clearly showed that rate the of decomposition of BF is higher than BF-M(II). BF and BF-Co(II) in that order show one and three thermal decomposition steps, while others undergoes two decomposition steps, indicating that strong interaction/chemical bonding exist between polymeric ligand and metal ions [33].

In BF polymeric ligand, thermal degradation starts from 50 °C and showed significance mass loss (~90 %) between 200 and 350 °C which are accompanied by removal solvents and cracking of polymer. There are three degradation peak temperatures in BF-Co(II). The first two peak temperatures T_{max1} and T_{max2} were due to thermal degradation of coordinated water molecules accompanied with evolution of the volatiles/removal of terminal groups. The last or third peak temperature T_{max3} shows the thermal decomposition of bridged methylene due to cracking of polymers and finally char-forming reaction in solid state. The first higher peak temperature T_{max1} in BF-Ni(II) polymer was occurred due to thermal degradation of coordinated water molecules accompanied with depolymerization reactions and second lower peak temperature T_{max2} due to thermal degradation of small molecular weight polymer fragments. BF-Cu(II) and BF-Zn(II) polymer complexes initially showed 4–5 % mass loss which support the absence of coordinated water molecules. The process of decomposition of both occurred as depolymerization, thermal decomposition of bridged methylene, and char-forming reaction. TG/DTG data clearly show that decomposition reaction of Zn-M(II) occurs at lower temperatures in regard to others.

Thermal kinetics investigation

The thermal decomposition of BF and its BF-M(II) is further elucidated by thermal kinetics studies. The plots of $\ln\beta$ versus $1000/T$ (FWO) and $\ln\beta/T^2$ versus $1000/T$ (KAS) corresponding to different degrees of conversion (α) (10–80 %) for heating rates of 10, 15, and 20 °C min^{-1} can

be obtained by a linear regression of least-square method, respectively, presented in Figs. (4, 5). A linear relationship is observed by both methods, and E_a can be evaluated from slopes of straight lines with better linear correlation coefficient (r^2 = 0.995–0.999). The dependence of apparent activation energy on degree of conversion ($E_a - \alpha$ curve) for non-isothermal decomposition process of polymers via FWO and KAS methods is presented in Fig. 6. From results obtained, the following remarks can be pointed out:

[i] It could be observed that approximately equal values of E_a are obtained by FWO and KAS methods, but with slightly lower E_a values calculated by KAS method. [ii] The initial thermal degradation process in BF and its BF-M(II) polymers showed that levels of E_a are different to each other, which involves a simple irreversible reactions because of removal solvents and volatile groups. Free radical formation takes place after initial step, which undergo inter-/intramolecular reactions, hampering thermal degradation process, or accelerating [34]. [iii] The E_a for BF increases with increasing α, while in case of BF-M(II) it increases on going from one decomposition stage to another indicating that rate of decomposition increases in same order. In case of BF-Co(II) and BF-Cu(II), final stage of conversion showed decreasing dependences and interpreted this fact as transition of process to diffusion-controlled reaction, rather than to follow the kinetic factor [35]. It was also observed that in BF-Cu(II) and BF-Zn(II), apparent activation energy showed quite opposite trend in the beginning, comparison to BF-Co(II) and BF-Ni(II). This may be attributed to structural rigidity, molecular mass, and type of metal ion influences.

As a consequence, variation in apparent activation energy with degree conversion is associated with heterogeneous process. Reactions occurred at a gas–solid interface, involved a multi-step parallel, consecutive, and irreversible reactions on thermal degradation process, and structural rigidity of polymers [10, 15, 35], which bonds different activation energies and mechanisms of thermal degradation [36], revealing to complex nature of decomposition process.

Conclusions

The new polymeric ligand was synthesized via condensation reaction of biuret with formaldehyde in basic medium. The polymer metal complexes of BF were synthesized with Co(II), Ni(II), Cu(II), and Zn(II). The results indicate that BF-Co(II) and BF-Ni(II) show octahedral geometry, while BF-Cu(II) and BF-Zn(II) show square planar and tetrahedral geometry, respectively. The apparent activation energy depends on degree conversion, so we observed that decomposition reaction process of prepared polymers precursor is a complex kinetic mechanism. This result shows the importance of isoconversional methods to evaluate apparent activation energy versus a without knowledge of kinetic model $g(\alpha)$ and shows that apparent activation energy evaluated by both methods is very good agreement.

Acknowledgements This project was supported by Deanship of Scientific Research, College of Science—Research Center, King Saud University, Riyadh, Kingdom of Saudi Arabia.

References

1. Yoshida M, Omichi H, Katakai R. Light-scattering study of temperature-responsive poly(acryloyl-L-proline methyl ester). Eur Polym J. 1992;28:1141–5.
2. Tsuchida E, Nishide H. Polymer-metal complexes and their catalytic activity. Adv Polym Sci. 1977;24:1–87.
3. Diab MA, El-Sonbati AZ, Ghoniem MM. Polymer complexes. IX. Thermal stability of poly[bis (2,6-diaminopyridine sulphoxide)] and polymer complexes of bis(2,6- diaminopyridine sulphoxide) with copper halides. Acta Polym. 1989;40:545–7.
4. Patel MM, Kapadia MA, Joshi JD. Synthesis, characterization and applications of coordination polymers of Ln(III). Appl Organomet Chem. 2008;22:689–97.
5. Marcu M, Cazacu M, Vlad A, Racles C. Chelate polymers, II. Some novel transition metals complexes with azomethine-containing siloxanes and their polyesters. Appl Organomet Chem. 2003;17:693–700.
6. Ahamad T, Kumar V, Nishat N. Synthesis, characterization and antimicrobial activity of transition metal chelated thiourea–formaldehyde resin. Polym Int. 2006;55:1398–406.
7. Nishat N, Ahamad T, Alshehri MS, Parveen S. Synthesis, characterization, and biological evaluation of semicarbazide–formaldehde ligand and its polymer metal complexes. Eur J Med Chem. 2010;45:1287–94.
8. Parveen S, Ahamad T, Nishat N. New antibacterial polychelates: synthesis, characterization and antibacterial activities of thiosemicarbazide–formaldehyde resin and its polymer metal complexes. Appl Organomet Chem. 2008;22:70–7.
9. Ebewele RO, Myers GE, River BH, Koutsky JA. Polyamine-modified ureaformaldehyde resins. I. Synthesis, structure, and properties. J Appl Polym Sci. 1991;42:2997–3012.
10. Wendlandt WW. Thermal methods of analysis. New York: Wiley; 1974.
11. Sestak J. Thermodynamical properties of solids. Prague: Academia; 1984.
12. Flynn JH, Wall LA. General treatment of the thermogravimetry of polymers. J Res Nat Bur Stand A Phys Chem. 1966;70A:487–523.
13. Ozawa T. A new method of analyzing thermogravimetric data. Bull Chem Soc Jpn. 1965;38:1881–6.
14. Kissinger HE. Reaction kinetics in differential thermal analysis. Anal Chem. 1957;29:1702–6.
15. Akahira T, Sunose T. Trans. Joint Convention of Four Electrical Institutes, Paper No. 246, 1969 Research Report, Chiba Institute of Technology Sci Technol. 1971;16:22–31.
16. Friedman HL. Kinetics of thermal degradation of char forming plastics from thermogravimetry. Application to a phenolic plastic. J Polym Sci C. 1964;6:183–95.
17. Coats AW, Redfern JP. Kinetic parameters from thermogravimetric data. Nature. 1964;201:68–9.
18. Erri P, Varma A. Diffusional effects in nickel oxide reduction kinetics. Ind Eng Chem Res. 2009;48:4.

19. Vyazovkin S, Sbirrazzuoli N, Dranca I. Variation in activation energy of the glass transition for polymers of different dynamic fragility. Macromol Chem Phys. 2006;207:1126.
20. Vyazovkin S. On the phenomenon of Variable activation energy for condensed phase reactions. New J Chem. 2000;24:913.
21. Brown ME, Maciezewski M, Vyazovkin S, Nomen R, Sempere J, Burnham A, Opfermann J, Strey R, Anderson HH, Kemmler A, Keuleers R, Janssens J, Desseyn HO, Li CR, Tang TB, Roduit B, Malek J, Mitsuhashi T. Computational aspects of kinetic analysis. Part A: the ICTAC kinetics project-data, methods and results. Thermochim Acta. 2000;355:125–43.
22. Burnham AK. Computational aspects of kinetic analysis. Part D: the ICTAC kinetics project-multi-thermal-history model-fitting methods and their relation to isoconversional methods. Thermochim Acta. 2000;355:165–70.
23. Doyle CD. Series approximations to the equation of thermogravimetric data. Nature. 1965;207:290–1.
24. Jada SS. The structure of urea–formaldehyde resins. J Appl Polym Sci. 1988;35:1573–92.
25. Kaliyappan T, Swaminathan CS, Kannan P. Studies on poly(2-Hydroxy-4- methacryloyloxybenzophe-none)-metal complexes. Eur Polym J. 1997;33:59–65.
26. West DX, Liberta AE, Padhye SB, Chikate RC, Sonawane PB, Kumbhar AS, Yerande RG. Thiosemicarbazone complexes of copper(II): structural and biological studies. Coord Chem Rev. 1993;123:49–71.
27. Prasath RA, Nanjundan S. Synthesis and characterization of metal-containing polyurethanes and polyurethane-ureas. Eur Poly J. 1999;35:1939–48.
28. Kelly PF, Slawin AMZ, Soriano RAJ. Reaction of $(Me_3SiNSN)_2S$ with palladium complexes-crystal structures of $[PPh_4]_2[Pd_2Br_4(S_3N_2)]$ and $[PPh_4][PdBr_2(S_2N_3)]$. Chem Soc Dalton Trans. 1996;1:53–9.
29. Hall IH, Chen SY, Barnes BJ, West DX. The hypolipidemic activity of heterocyclic thiosemicarbazones, thioureas and their metal complexes in Sprague dawley male rats. Met Based Drugs. 1999;6:143–8.
30. Konig E. Structure and bonding. Berlin: Springer; 1971.
31. Ibrahim Y, Alaaddin C. Synthesis, characterization and antimicrobial activity of the Schiff bases derived from 2,4-disubstituted thiazoles and 3-methoxysalicylaldehyde, and their cobalt(II), copper(II), nickel(II) and zinc(II) complexes. Trans Metal Chem. 2003;28:399–404.
32. Ahamad T, Nishat N. New antimicrobial epoxy-resin-bearing schiff-base metal complexes. J Appl Polym Sci. 2008;107:2280–8.
33. Hatakeyama T, Quinn FX. Thermal analysis: fundamentals and applications to polymer science. 2nd ed. Chichester: Wiley; 1999.
34. Sodhi GS. Correlation of thermal stability with structures for some metal complexes. Thermochim Acta. 1987;120:107–14.
35. Loitescu A, Vlase G, Vlase T, Doca N. Thermal behaviour of some industrial and food dyes. J Therm Anal Calorim. 2007;88:121–5.
36. Gongwer PE, Arisawa H, Brill TB. Kinetics and products from flash pyrolysis of cellulose acetate butyrate (CAB) at 460–600 °C. Combust Flame. 1997;109:370–81.